

# MATERIAL COMPOSITION OF ORES AND METASOMATICALLY ALTERED ROCKS AT BEREZNYAKOVSKOE EPITHERMAL GOLD ORE DEPOSIT (THE SOUTH URALS)

Spiridonov A.M., Kulikova Z.I., Zorina L.D., Granina E.M., Parshin A.V., Budyak A.E.

Institute of Geochemistry named after Vinogradov A.P., the Siberian Branch of Russian Academy of Sciences  
1a Favorsky Str., Irkutsk, 664033

Bereznyakovskoe epithermal gold ore deposit is situated within Birgildinsko-Tominsky porphyry-copper ore cluster; it is located in the upper side of vertically extended porphyry-copper chute. The deposit is confined to a subvolcanic body of quartz-plagioclase diorite porphyry ( $D_3-C_1$ ) that transects andesite dacitic tuffs and clastic lava of sedimentary volcanic rock mass ( $D_3-C_1$ ) forming a single volcanic-plutonic assemblage. Vein and disseminated gold ores, as well as stockworks are located in linear sublatéral and north-westward trending areas. Pre-ore chlorite-carbonate-mica-quartz-albite and further chlorite-carbonate propylites are discovered in the halo selvages of altered rocks; also, argillization is discovered. Mineralization is accompanied by mica-quartz, pyrophyllite-quartz and rarely carbonate-mica-quartz metasomatites.

As per material composition, the ore is illite-pyrophyllite-quartz, mica-quartz with scattered fine grained impregnations, as well as vein impregnations and clusters of pyrite (9.2 %) mainly. Proportion of fahlores with admixture of secondary copper sulfides is 0.6% and admixture of sphalerites is 0.4%.

The bulk of the stated ore minerals in the sample characterizing ordinary primary ores of the central part of the deposit can be referred to the telluride-polymetallic period (telluride-fahlore and gold-telluride sub-periods). There is inessential presence of ores of enargite sub-period, and galena-sphalerite and quartz-carbonate periods of mineralization. The bulk of gold is in the native high-purity and pure forms, the smaller part of gold is related to gold tellurides. Often, gold intergrowths with sulfides, sulfosalts, as well as with quartz, pyrophyllites, sericites, and illites.

## Introduction

Discoveries of recent years have considerably changed knowledge about gold metallogeny of the Urals. Here new origin types of gold deposits were discovered; among them are Vorontsovskoe deposit of carlin type (Sazonov et al., 1998) and Bereznyakovskoe deposit of epithermal type (Grabezhev, Moloshag, 1993; Sazonov et al., 1994; Grabezhev et al., 1995; Lehmann et al., 1999). This knowledge greatly enhances the prospects of the Urals as a gold mining region. All this served as the basis for starting more detailed mineralogical and geochemical studies of the material composition of ores and metasomatically altered rocks of Bereznyakovskoe epithermal gold deposit. The deposit is located 20 km south-westwards of Chelyabinsk within Birgildinsko-Tominsky ore cluster, which is located in the south of the exocontact of Chelyabinsk polychronous (C1-P) granitoid pluton in the area of intersection of the East Ural volcanic zone with the East Ural uplift.

The top issue of the modern stage of gold deposit development is a more complete recovery of commercial component. Bereznyakovskoe deposit is one of attractive areas for development of the innovative ore processing technologies, at which additional detailed study of mineral composition of ores and enclosing rocks would allow enhancing efficiency of the processing flowsheet and gold recovery at this mining object.

## Geological Composition and Mineralization of Bereznyakovskoe Deposit

Bereznyakovskoe epithermal gold ore deposit is situated within Birgildinsko-Tominsky porphyry-copper ore cluster; it is located in the upper side of vertically extended porphyry-

copper chute. The mesoabyssal section of the latter directly corresponds to the mesoabyssal section of North-Tominsky deposit [Grabezhev et al., 2000; Korobeynikov, Grabezhev, 2003]. Due to block-tectonic composition of the ore field, at the present moment the deposits are located within the same erosion section but in the different tectonic blocks: North-Tominskoe in basalts of the lower structural stage (O1-2), and Bereznyakovskoe in the sedimentary-volcanic strata of the upper structural stage (D3-C1).

Geological and origin status of Bereznyakovskoe deposit in the zoning scheme of the gold-copper-porphyry chute corresponds to the existing theoretical concepts [Lowell, Guilbert, 1970 et al.] and is confirmed by the correlation of the deposit with subvolcanic intrusion of diorite porphyries, isotopy of O, S and C, and the results of barothermal and geochemical researches [Taylor, 1982; Sillitoe, 1992; Hedenquist et al., 1996, 1998; Grabezhev et al., 2000]. The deposit corresponds to the vertical and lateral zonation of large porphyry copper deposits [Einaudi, 1977; Krivtsov et al., 1985, 1986; Bartos, 1989; Sillitoe, 1992; Rusinov et al., 1993; Hedenquist et al., 1996, 1998; Grabezhev et al., 2000] and is the product of a single porphyry-epithermal fluid-magmatic system, similar to those as Darasunsky, Carian and Baley gold ore-magmatic systems are the products of a single porphyry-epithermal systems of the Eastern Transbaikalia [Prokofyev et al., 2010].

The geological structure of Bereznyakovskoe deposit includes subvolcanic body of quartz-plagioclase diorite porphyries (D<sub>3</sub>-C<sub>1</sub>), that transects andesite-dactic tuffs and clastic lava of sedimentary-volcanic strata (D<sub>3</sub>-C<sub>1</sub>) forming a unite volcano-plutonic assemblage with them (Fig. 1).

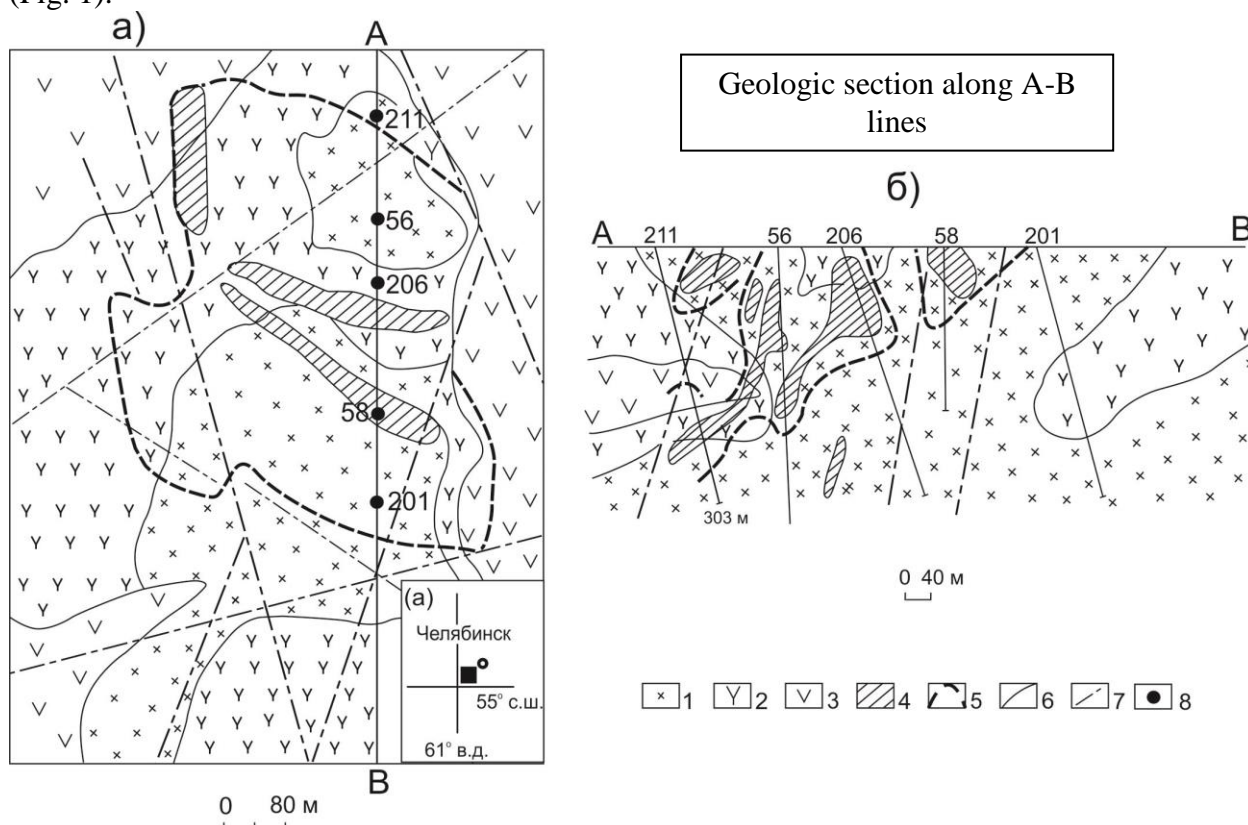


Fig. 1. Schematic geological map (a) and geologic section (b) of Bereznyakovskoe deposit (according to Grabezhev et al., 2000)

1 - quartz diorite porphyry; 2 - subvolcanic quartz andesite porphyry; 3 – tuffs of sedimentary-volcanic strata D3-C1; 4 - ore bodies; 5 – borders of the ore zone (Fig. 1a) and zones of moderate white mica formation (usually in association with chlorite) without carbonate (Fig. 1b); 6 - geological boundaries of rocks; 7 - tectonic faults; 8 - boreholes; 9 - location of Bereznyakovskoe deposit.

Two sites of Berezhnyakovskoe deposit are the most thoroughly explored; they are the Central site and the South-Eastern site [Plotinskaya et al., 2007]. Contoured ore bodies with vein-disseminated mineralization are predominantly located in the body of intensively cataclased, mylonited and schistosed diorite porphyry. They are confined to the central part of the metasomatic halo of acid leaching represented by chlorite-mica-quartz-albite metasomatites with thickness up to 200m. Among them are bodies of mica-quartz and pyrophyllite-quartz metasomatic rocks ranging from 1-2 to 60 m [Grabezhev et al., 2000]. Pyrophyllite-quartz metasomatic rocks conjugate with ore bodies. Mica of tectonic metasomatite schistosity zones is represented by hydroparagonites and paragonite-smectites containing 11-27% of montmorillonite layers; at that, the latter are formed later in the process of hypogene hydration, overlapping potassium and sodium mica. Chlorite-carbonate-mica-quartz-albite and chlorite-carbonate propylites developed in the selvage of the altered rocks halo.

Vein-disseminated gold ores are located in linear areas of sub-lateral and north-west extension, as well as in stockworks [Grabezhev et al., 2000]. Ore bodies are characterized by extremely irregular thickness and variable gold contents; their form is elongated linear, often winding, lens or column type; their length reaches 300 m, and their thickness varies from 0.3 m to 92.0 m. Sublatitudinal and north-west strike of the ore bodies prevails at steep northward and northeastward falls (40°-80°). Gold content in the ore bodies varies from 1 to 59 g/t, silver content – from 3 to 40 g/t. High concentrations of Cu, Zn, Ag, Sn and high contents of Pb, As, Sb, Se, Te are discovered in the zones of gold ore bodies.

### Metasomatic Alteration of Enclosing Rocks

According to petrographic studies of altered enclosing rocks it was stated that the rocks are represented by metasomatites of mica-quartz, pyrophyllite-quartz and rarely carbonate-mica-quartz composition. Relic porphyric and blastoporphyr texture remains during metasomatic alterations; at that, original feldspars were almost completely replaced. There are two types of metasomatites according to their structural features: the one with prevailing microgranular structure replaced by secondary products of the bulk mass supposedly formed above quartz andesite porphyry or above quartz diorite porphyry in their body selvage where rocks are less decrystallized (Fig. 2a, 2b), and the one with more coarse grained structure formed on quartz diorite porphyry (Fig. 3a, 3b). The rocks are cataclised and friable. The less altered rocks contain single porphyry impregnations of quartz; porphyry impregnations of plagioclase (45-50%) are supposedly completely replaced by micro-scale mica aggregate, only its contours remains; plagioclase grains are also replaced in their bulk (all in all, mica aggregate may total up to 65-70%). According to the results of X-ray structural analysis, performed at the SB RAS Institute of Geochemistry named after A.P. Vinogradov, mica is represented by pyrophyllites; hydromica illite represents clay minerals.

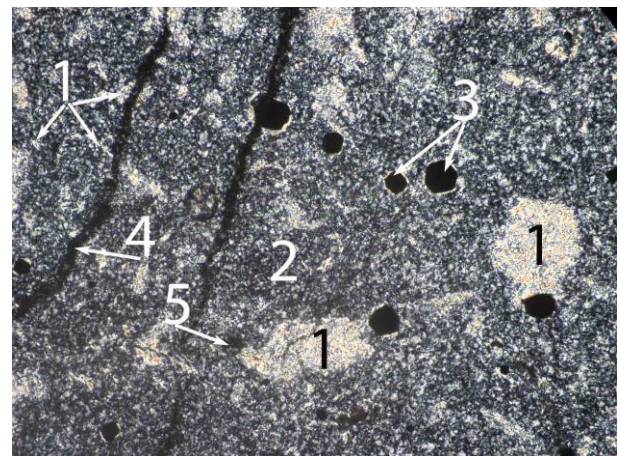
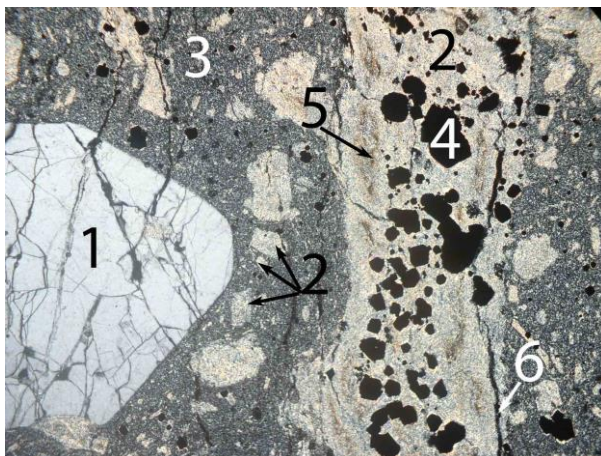


Fig. 2. Thin section. Metasomatite of mica-quartz structure with abundant inclusions of pyrite. A. 1 – porphyritic quartz phenocrysts; 2 – micro-scale mica aggregate with illite prevailing and having replaced the feldspar in its bulk mass and its porphyritic phenocrysts; 3 – fine grained quartz aggregate with mica scales impregnations; 4 – pyrite impregnations confined to mica aggregate clusters (along replaced phenocrysts); 5 – hydroxides of iron; 6 - ore material on the cracks. Field of view is 4 mm. Nicoli +. B. The bulk mass. 1 - small porphyritic phenocrysts and grains in the bulk completely replaced by mica aggregate with illite prevailing; 2 - fine grained quartz aggregate with mica scales impregnations; 3 – pyrite impregnations; 4 – cracks filled with ore material; 5 - defects in thin section. The field of view is 0.8 mm. Nicoli +.

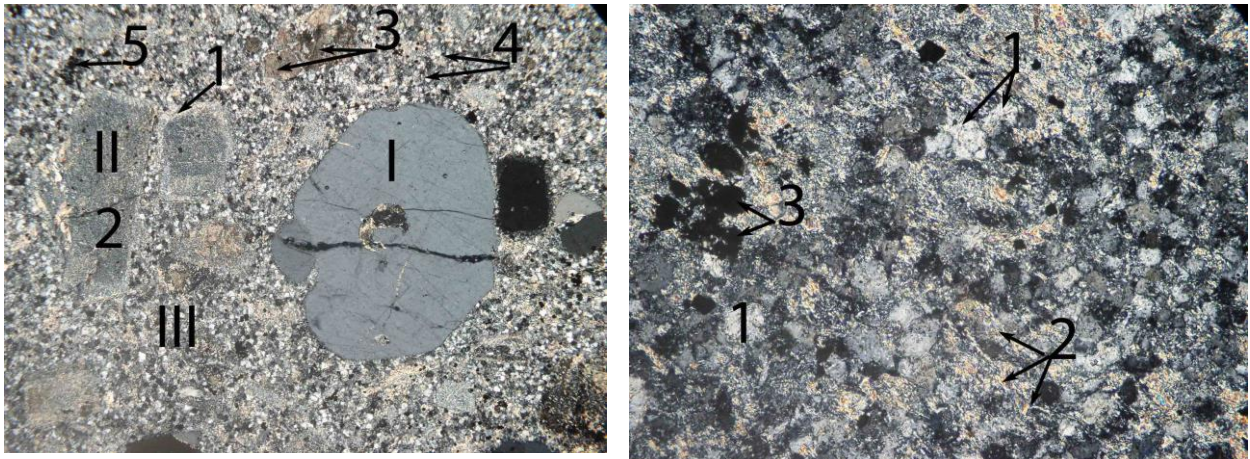


Fig. 3. Thin section. Metasomatite of carbonate-mica-quartz structure formed on quartz diorite porphyry. A. I – porphyritic quartz phenocrysts; II – completely replaced porphyritic phenocrysts of feldspars and biotites; III – replaced bulk mass; Minerals: 1 – pyrophyllite scales (?) along the edges of porphyritic phenocrysts; 2 – micro-scale clay-micaceous mass (illite, etc.); 3 – carbonate; 4 – bulk fine grained quartz; 5 – fine grains of ore minerals. Field of view is 4 mm. Nikoli+. B. The bulk mass. 1 - fine isometric grains of quartz; 2 – micro-scale mica aggregate (illite, pyrophyllite?); 3 - crystals of pyrite. The field of view is 0.8 mm. Nicoli +.

In the bulk (45-50%) fine grained quartz aggregate prevails with slight mica impregnations having replaced plagioclases (size of quartz gains is 0.002 mm and less, in coarser grained type of metasomatites their size is 0.05 mm in diameter). Abundant pyrite impregnations tend to replace mica-plagioclase clusters. The texture of the bulk mass is microlepidogranoblastic, or blastohypidiomorph granular, or blastoaplitic.

Breccia is also present; it consists of fragments of mica-quartz metasomatites, fine grains of ore minerals and mica aggregate strips are formed along the boundaries of fragments. More intense formation of carbonates is observed in tectonic zones; their clusters total about 45-50% of the thin section; also, carbonate veinlets with up to 5 mm thickness and chlorite-pyrite-limonite-quartz-carbonate veins are found. Carbonate replaces pseudomorphs of mica aggregate formed along feldspars. Number of clay minerals rises in such areas.

Under more intense alterations outlines of porphyritic phenocrysts are smoothed and disappear; micaceous aggregate begins to develop in a form of numerous strips confined to microcracks (fig. 4a, 4b). Ore mineral impregnations are also confined to these microcracks, and such impregnations tend to be more abundant. Size of mica scales (pyrophyllite) increases, and admixture of clay components falls. The texture of rocks is glomero-blastic; the texture is microlepidoblastic in mica aggregate clusters and strips and microlepidogranoblastic in siliceous aggregate with predominant quartz grains (0.001-0.004 mm) and rare mica scales.

It seems that pyrophyllite formed later than illite, having replaced the latter; that means that argillization process typical for epithermal gold deposits was more previous and, obviously,

pre-ore one. Previous researchers noted muscovite, paragonite and K-Na-intermediate mica, often hydrated. Sodium mica is more common in the western part of the deposit [Grabezhev et al., 2000; Korobeynikov, Grabezhev, 2003], their content in the process sample studied by us is very small.

Pyrophyllite-quartz metasomatic rocks have the following composition: fine grained quartz aggregate (45-50%), spherulite-like aggregates of pyrophyllite, supposedly, with sizes ranging from 0.01 mm to 0.06 mm, forming fine chaotic conglomerations (45%), coarse grains of quartz, that can be relics of porphyric phenocrysts, ore formations, among which pyrite (5%) and other sulfides (2-3%) (Fig. 5). The texture is heteroblastic and glomeroblastic. Spherulite aggregates of pyrophyllite include fine crystals of pyrite.

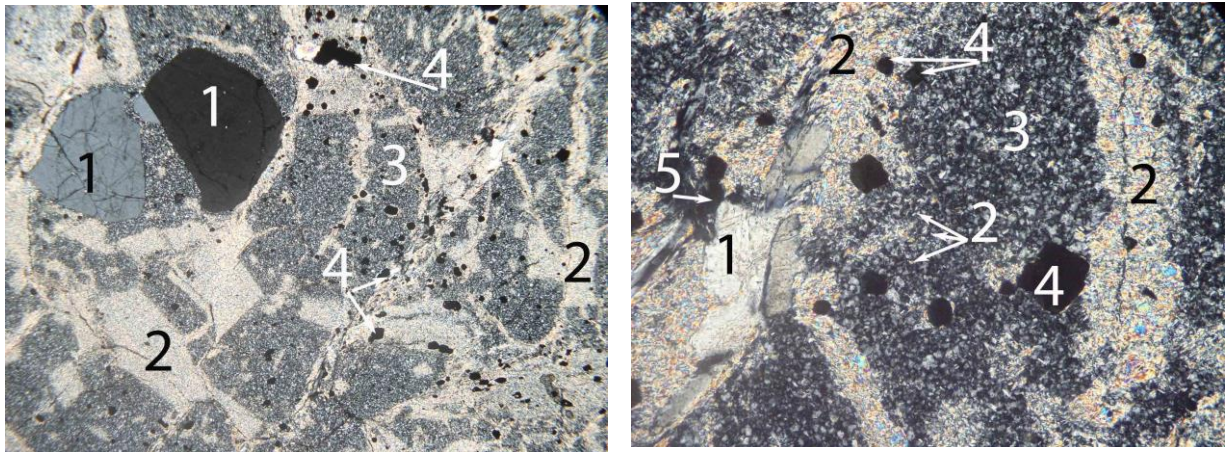


Fig. 4. Thin section. Metasomatite of mica-quartz structure with inclusions of pyrite. A. 1. – relics of porphyric phenocrysts of quartz; 2 – mica aggregate that replaced porphyric phenocrysts and bulk feldspar grains, formed along the cracks with pyrite and quartz; 3 – fine grained quartz aggregate along the bulk mass and single mica scales; 4 – pyrite impregnations. Field of horizontal view is 4 mm. Nicol +. B. The same rocks under higher magnification. 1 - secondary quartz developed along fractures with pyrite, pyrophyllite and illite; 2 – micro-scale pyrophyllite and illite, confined to cracks and replacing feldspars in their bulk; 3 – fine grained silica aggregate with mica scales; 4 - fine pyrite impregnations; 5 - cavities. The field of horizontal view is 0.8 mm. Nicol +.

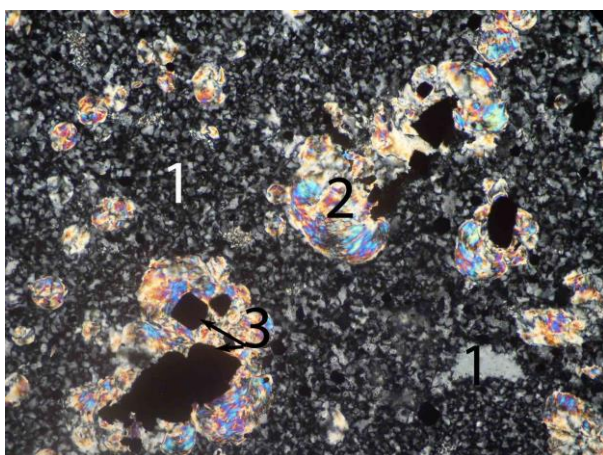


Fig. 5. Thin section. Pyrophyllite-quartz metasomatite with sulfide mineralization. 1 – fine grained quartz aggregate with mica admixtures; 2 – rosette-like, spherulite-like aggregates of pyrophyllite; 3 – pyrite. The field of horizontal view is 0.8 mm. Nicol +.

Moderately sulfide mineralization in the metasomatic rocks is observed in the form of scattered impregnations, thin vein-disseminated and spotted (clustered) outwards of mainly pyrite with admixture of fahlores, sphalerite, and lead sulfide.

Mica of shearing and crushing zones is often represented by hydraparagonite and paragonite-smectites replacing original mica (Grabezhev et al., 2000). Thermodynamic parameters of mica-quartz metasomatic rocks formation are the following:  $T = 380-320^{\circ}$ ,  $P = 0.8-1.2$  kbar, ore association (gold, electrum, tellurium; Au, Ag, Pb, Bi tellurides) formed at  $T = 260-360^{\circ}$  and  $P=0.1-0.4$  kbar; montmorillonization of mica occurred at  $T = 160-240^{\circ}$  and  $P = 0.1-0.4$  kbar (Grabezhev et al., 2003).

### **Features of Material Composition of Ores**

According to the results of previously conducted studies [Grabezhev et al., 2000] it was found that mineralization of Bereznyakovskoe deposit was formed in two stages: early pyrite and late polymetallic stages. Pyrite of the first stage is well developed both within the ore bodies, and outside them, conjugated with metasomatic altered rocks. Polymetallic stage can be observed throughout the stringer zones of silicification and carbonation, thus revealing significant variations of mineral composition. Three paragenetic associations of ore minerals can be distinguished; they are gold-polymetallic, gold-telluride-polymetallic and telluride-polymetallic. Quantitatively, all main minerals of these three parageneses are represented by fahlore, sphalerite, chalcopyrite, pyrite and galena. There is native gold of two generations typical respectively for the gold-polymetallic and gold-telluride-polymetallic parageneses [Korobeynikov, Grabezhev, 2003].

According to other, more recent data, three ore stages were identified [Plotinskaya, 2007]; they are pyrite (pyrite disseminated in quartz-sericite metasomatic rocks), the main ore, or telluride-polymetallic, and galena-sphalerite stages. Three substages can be distinguished within the main ore stage: enargite, fahlore-telluride and gold-telluride substages [Plotinskaya et al., 2007].

According to the results of X-ray analysis (Table 1) the bulk of the primary ore sample consists of quartz, pyrophyllite, illite, sericite, paragonite, and of ore minerals - pyrite, fahlores, sphalerite, galena, chalcopyrite, in descending order respectively. Pyrite predominates among ore minerals; its share in the sample totals up to 10 ppm %. The total share of copper minerals - fahlores, secondary copper sulfides, sulfosalts – is about 0.6 ppm %. Sphalerite is not more than 0.4 ppm %, galena is about 0.1-0.15 ppm %. Commercial components (gold and silver) are represented by native gold, as well as accumulated in gold tellurides, silver tellurides, and

slightly less in fahlores.

**Table 1. Mineral composition of the original ore sample**

Minerals and mineral groups	Mass fraction, %
<b>Rock forming and vein minerals:</b>	
Quartz	35-40
Micaceous and hydromicaceous (pyrophyllite, illite, sericite, paragonite) Rarely chlorite	50
Plagioclase (albite)	< 0,5
Carbonate (ankerite)	1,0
<b>Ore minerals:</b>	
Pyrite	9.2
Gray ores (tennantite, tetrahedrite, telluride fahlore), less - secondary copper sulfides	0.6
Sphalyrite	0.4
Galenite	Particles
Chalcopyrite	Occasional particles
Hydroxides of iron	Particles (less than 0.2-0.5 %)
Apatite, sphene, leucosene, zircon	Particles and occasional particles
Gold, silver	Particles

*Quartz* is represented by automorphic and hypautomorphic grains and their intergrowths with micaceous minerals and sulfides in the sample. The size of grains reaches up to 1.0-2.0 mm.

Micaceous and hydamicaceous pyrophyllites, illites, sericites, and small amount of paragonites are present in the form of independent fine prismatic and schistose grains and aggregates, in the form of intergrowths with quartz and sulfides. Besides, illite and sericite are discovered in the form of complete plagioclase pseudomorphs (albite). Sizes of micaceous minerals in intergrowths range in two and three decimal places of the millimeter.

*Carbonates* (mainly ankerite) occur as isolated small grains and fine-grained aggregates. Intergrowths with host minerals - quartz, mica, chlorite – are frequent. Weak limonitization is rarely observed by carbonates.

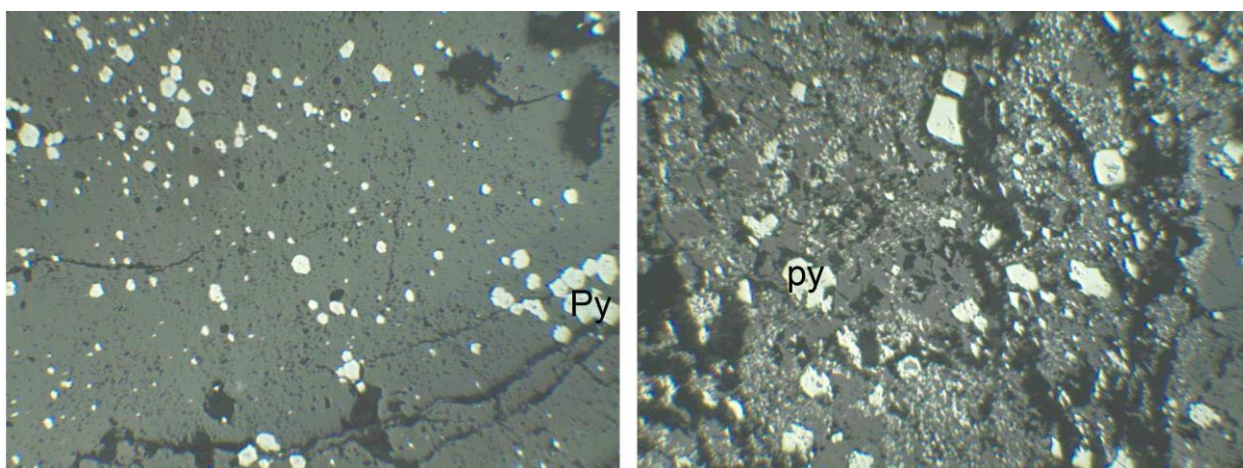


Fig. 6. Polished ore. A. Impregnated framboidal outwards of pyrite in quartz-mica metasomatic rocks. B. Fine-grained porphyroblastic texture of pyrite in meta-vein quartz outwards in quartz-mica metasomatic rocks. Microscope. The field of view is 2.4 mm. Nicholi II.

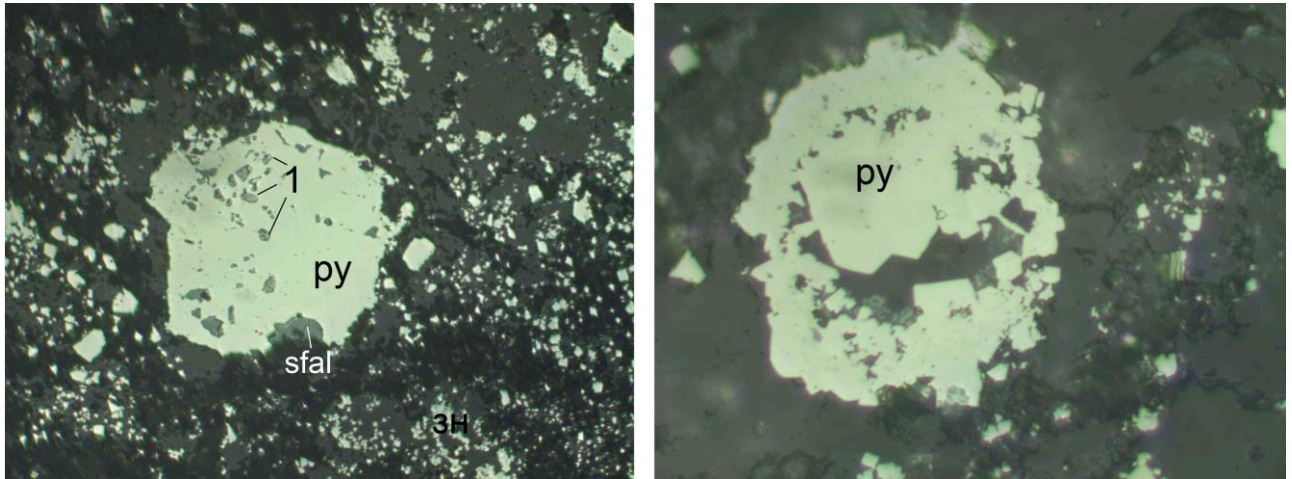


Fig. 7. Polished ore. A. Quartz-mica metasomatic rocks; fine-grained, porphyroblastic texture of pyrite. B. Openwork spherical pyrite aggregate. II. Microscope. Nicholi II. Field of view: A - 0.6 mm; B - 0.15 mm.

As it was stated above, pyrite forms the bulk mass of sulfides. It develops in the form of impregnations, or spotted clusters of grained porphyroblastic aggregates, or spherical and openwork clusters (Fig. 6, 7). Grain sizes vary from three decimal places of mm to 0.5 mm. The most common sizes of grains and aggregates are less than 0.1-0.05 mm, up to 1-5 micron (II generation). Grain forms of pyrite are automorphic, hypautomorphic (pyritohedron, cubes and their combinations), framboidal. Porphyroblastic, poikilitoblastic, cribrose and micropoikilitic textures with quartz impregnations and rarely with galena, chalcopyrite or fahlore impregnations are typical. Cancellated zone structures were found (according to lamination of coarse grains); sometimes their central parts are filled with quartz. According to its material composition, pyrite is enriched with sulfur S (55.2%). Pyrite sometimes is enriched with arsenic (about 1%) along grains and aggregate periphery, along cracks and growth zones. Pyrite grains and aggregates are cataclastic and corroded with micaceous minerals and carbonates in shear and veinlet development zones. Aggregates of silicates (quartz, mica minerals, mostly pyrophyllite), fahlores, sulfosalts and sphalerite are found along cracks and periphery. Fine impregnations of galena, fahlores, enargites, chalcopyrites, tellurides, selenides, titanium oxides and gold (less than 1-5 micron) are discovered in pyrite (Fig. 8, Table 2). Fine crystal grained outwards of pyrite were in its turn found in fahlores, secondary copper sulfides; they also transect sphalerites. According to the data of Plotnitsky O.Y. [2006] the studied pyrite can be referred to pre-ore and ore stages, i.e. I and II generations.

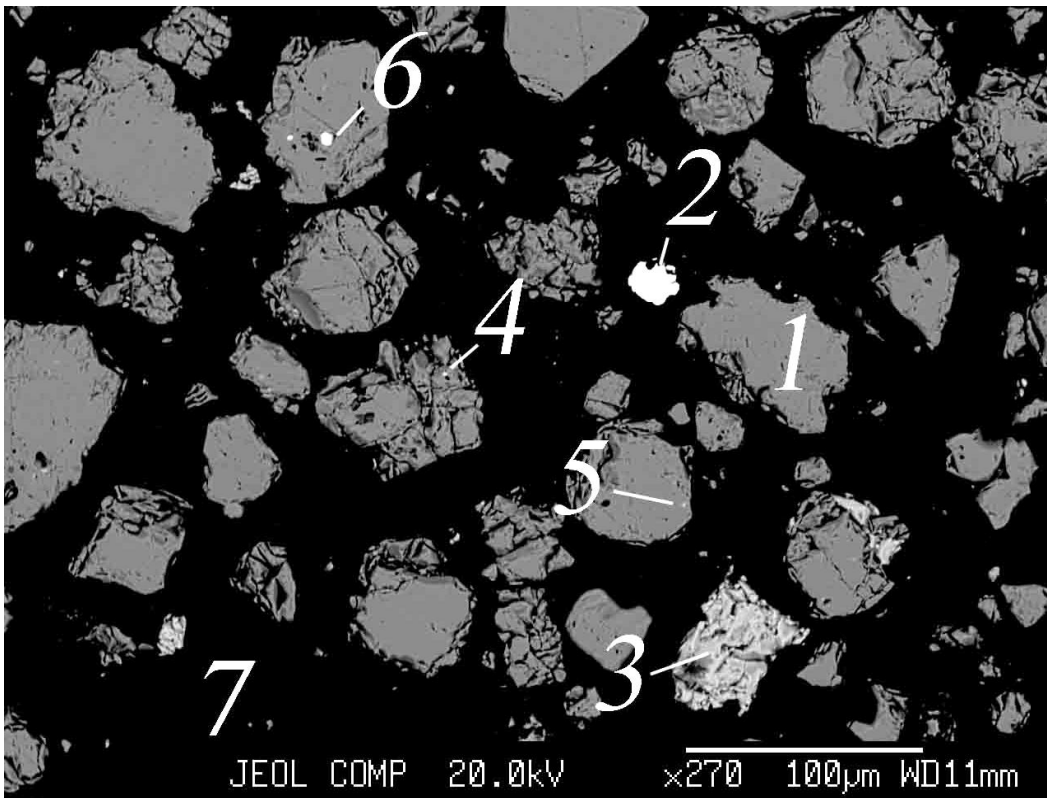


Fig. 8. Briquette flotation concentrate polished section. Among fragments of pyrite (1, gray) there a subtle grain of gold (2 white), fahlore (3, tennantite) are observed. Thin inclusion of gold (4), tennantite (5), less than 1.2 microns, and galena (6), less than 5 microns are visible in pyrite. 7 - balsam (cement). Backscattered electrons.

**Table 2. The composition of thin inclusions in pyrite of quartz-sulfide flotation concentrate from the original ore. Microprobe analysis.**

No.	Elements, weight ratio, %									Mineral
	Ag	Pb	Te	Cu	Se	Sb	As	S	Fe	
6	10.36		51.49							<b>Au - 38,16</b> Relative to sylvanite
7		60.87	21.58			4.85		12.70		Galena with altaite, Sb admixture
8		35.11			57.46			6.12	1.31	Clausthalite (PbSe), part of Se is presumably in native form
9		100.00								Native lead
10	11.50			31.40		6.00	18.80	31.80		Silver bearing fahlore

*Chalcopyrite* is identified in microcracks in the form of thin xenomorphic inclusions, mainly in pyrite. It is in association presumably with fahlores and sphalerite.

*Fahlores* are most common after pyrite. According to frequency fahlores are more predominant, and minerals of sulfosalts of famatinite-luiconite group and enargites are less frequent in compliance with microprobe analysis of original ores and their flotation concentrates (gold-quartz, copper-containing, pyrite). Fahlore outwards are in the form of xenomorphic and fine-veinlet aggregates; they are often located along cracks, interstices and along pyrite aggregate periphery in the form of fine inclusions. Fahlores are associated with sphalerites, together corroding pyrite. Inclusions of tellurides (fig. 9) are discovered in fahlores.

Fahlores are heterogeneous by their composition. They are represented mainly by tennantite, and gray copper in single cases; the latter is found in tennantite in the form of stripes and spots (bleached in backscattered electrons). Detailed description of fahlores was performed by Plotnitskaya O.Y. [2007], who has stated four generations of fahlores. According to the results of microprobe analysis variation limits of main elements in arsenious fahlores (tennantite) are the following (weight ratio, %): Fe 0.47–6.56; Cu 31.89–42.8; Zn 1.35–7.53; S 26.89–33.36;

As 15.47–25.46; Sb 4.26–13.23; in antimony fahlores (grey copper): Fe 0–3.57; Cu 33.89–37.83; Zn 4.84–8.98; S 25.88–27.00; As 6.38–12.97; Sb 11.57–21.69. Constant presence of zinc is the main feature. Separate fine aggregates of silver-bearing (Ag up to 11.5 ppm %, Table 2) and bismuth-bearing fahlores (Bi – 22.03 ppm %, admixtures are about 1.5-3.9%) were discovered. Admixture of molybdenum was discovered in a single case (up to 5.1%). Hypogene replacement of fahlores by secondary copper sulfides is observed. According to their material composition secondary copper sulfides are relative to digenites, covelline and girites (Cu ratio totals 56.60-74.62; Fe varies from 0.87 to 1.8 ppm %). Secondary sulfides develop in the form of aggregates of crumbled and cellular structure throughout the fahlore outwards, as well as in the form of vein, zonal, openwork and limbic aggregates throughout fahlores, sphalerites and sometimes galena.

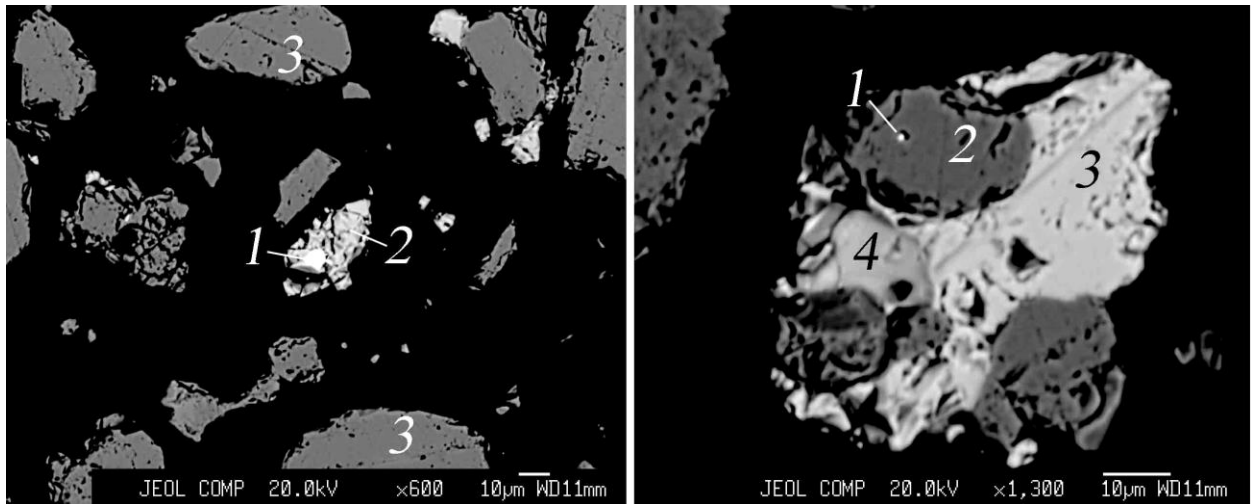


Fig. 9. A - Oval altaite inclusions (1) of 7-10 microns size in fahlore (2). 3 - pyrite aggregates. b- fine inclusions of galena (1) with altaite (<1 micron, white) in pyrite (2, gray), pyrite (2) intergrowths with fahlores (3, light gray) and sphalerite (4, gray). Backscattered electrons.

Complex sulfosalts were discovered; according to their material composition they refer to iron-antimony oxisalts, supposedly, valleriite group.

*Antimony and arsenic sulfosalts* of famatinite-lyuconite type (determined by X-ray analysis) are less common than fahlores; they are reported in association with fahlores, sphalerite and pyrite; they retain high proportion of zinc up to 10.3% (as fahlores).

Sphalerite associates with pyrite and fahlores; secondary Cu minerals often develop along cracks and sphalerite aggregate periphery (see Fig. 10). The grain size of spotted and vein sphalerite aggregates varies from 1-10 micron up to 100 micron (single grains). Sphalerite is often isomorphic to fahlores; grains with partial and complete hexagonal limitations are found. In bulk material composition of sphalerite is rather homogeneous and is close to theoretical concepts. Weight ratio (in % for all elements stated) of Zn varies in the range from 58.87 to 62.75, under average value of 61.16; S varies from 33.16 to 35.59, average value is 34.82; Fe varies from 0.0 to 2.2, average value is 0.8; Cu fraction is rather high and varies from 1.49 to 5.77, its average value is 3.23. Sphalerite is low-iron one, sometimes there are As (9.57) and Sb (18.53) admixtures are stated. It is copper impregnated; there are zones of Cu (up to 35.51) and Zn (up to 41.97). Like fahlore outwards, sphalerite is also transected with fine cracks along which fahlores and secondary copper sulfides develop.

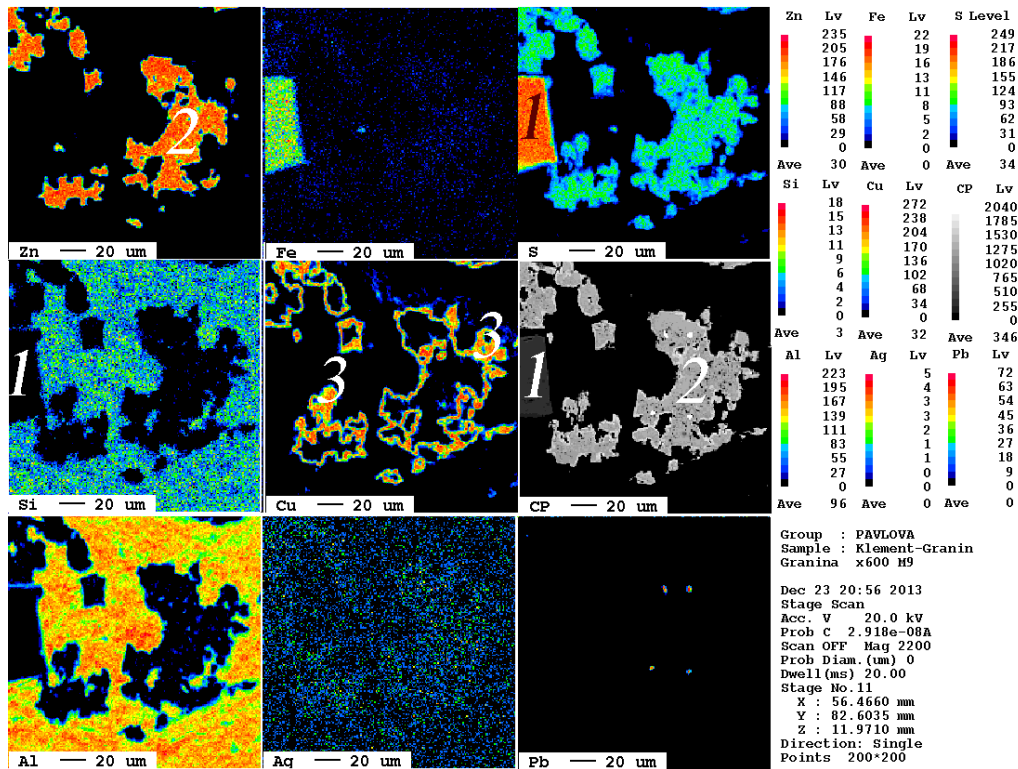


Fig. 10. Pyrite (FeS, 1) in association with sphalerite (2) in quartz-feldspar-mica mass. Digenite with covellite (3) form rims around sphalerite. Images are X-ray. CP - backscattered electrons. To the right changes in intensity of X-rays of a given element (from black - minimum to red - maximum) are stated.

Thin oval inclusions in pyrite (Fig. 11) and fahlores are characteristic for *galena*. There are intergrowths with gold tellurides and native silver (Fig. 11b). Composition of galena inclusions in pyrite are shown in Table 2. The most common are associations of galena with lead tellurides (altaite); presence of native tellurium is possible. There are associations of galena with selenides (clausthalite) and with native selenium supposedly. Altaite is present in galena in the form of impulsive intergrowths. Galena inclusions are less than 20 micron, the size of altaite and clausthalite inclusions is 10 micron and less. Material composition of plumbum tellurides and clausthalite is close to theoretical concepts (Table 3). Presence of Fe and S is observed in case of matrix overlapping. Native lead is present.

**Table 3. The results of microprobe analysis of plumbotellurides and selenide from quartz-pyrite flotation concentrate of original ore**

No.	No. eds_sqrt	Elements, weight ratio, %				Minerals, aggregates
		Pb	Fe	S	Te	
1	77_1	82.10	3.10	14.70		Galena with pyrite inclusions
2	94_6	48.90	8.63	10.00	32.40	Altaite, matrix intake (pyrite)
3	95_7	54.40	5.30	5.60	34.70	Altaite, matrix intake (pyrite)
4	96_8	45.20	10.83	13.10	30.90	Altaite, matrix intake (pyrite)
5	97_9	67.72			32.30	Altaite (in galena)
6	140	70.91			29.08	Altaite and galena? (in pyrite)
7	197	64.79			35.21	Altaite (in intergrowth with galena and

						enargite)
8	203	62.95			37.05	Altaite (in intergrowth with pyrite)
9	264	62.68			37.31	Altaite (in fahlore)
11	257	70.37			29.63	Altaite (~1mkm) on the boundary of pyrite and tennantite
12	53*	72.00		8.00	Se -17.06	Galena and clausthalite

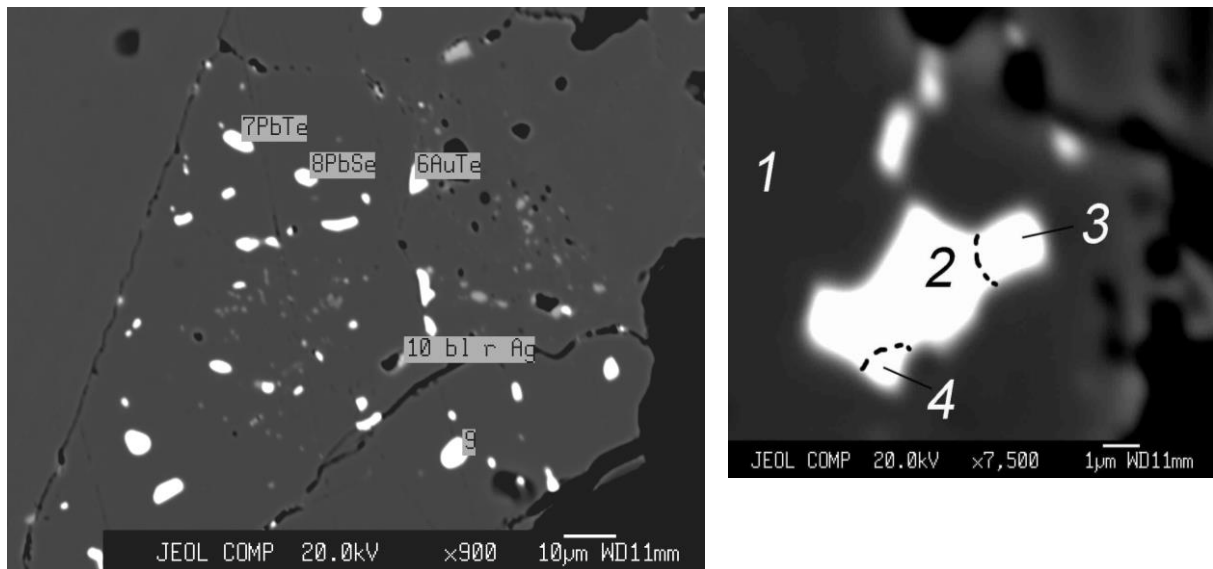


Fig. 11. A. Inclusions of gold telluride (sylvanite? Spot 6), lead stibiosulfotelluride (spot 7) krennerite (spot 8), native lead (spot 9), silver tennantite (spot 10) in pyrite. B. Galena aggregate (2, white) is observed in pyrite (1, dark gray). It is observed in the intergrowth with gold telluride (3, white) and, possibly, with native silver (4, white). Backscattered electrons.

The main commercial element of original ores is *gold*. According to the results of assaying, average content of gold in the ore is 2.4 g/t. The bulk of gold is in the native high-pure and pure forms (Fig. 12a). Some gold is in the form of gold tellurides (Table 4). According to size distribution analysis the gold is ultra-fine-grained (less than 0.05 micron); at that, fraction of fine-grained gold of 3-25 micron size is about 10% [Lodeyschikov, Vasilyeva, 1997]. Isometric segregations of gold with irregular edges is observed; the structure of grains is ultra-fine, of 17x20 micron size. Grid measurements were performed to determine chemical composition and distribution of elements in the gold aggregate (Fig. 12b). Variations of gold fraction in the aggregate of the discovered grain are inconsiderable (from 94.776 to 99.938 ppm %, average Au gold composition 98.4 ppm %); admixture of Fe from 0.062 to 5.25 ppm% is observed. Besides, composition of the gold is pure (Au 100 ppm %) and rather high-pure, or almost pure (Au 94.34; Ag 5.66 ppm%). Mass fraction of gold in tellurides is from 11 to 29%. Slight inclusions of quartz, aluminosilicates and titanium oxides are discovered.

The bulk of gold is in intergrowths with sulfides, sulfosalts, as well as with quartz, pyrophyllites and hydramicaceous minerals (sericite, illite). There is no gold free of intergrowths (amalgamable) in the ore, according to rational assaying. 80% of gold of the original ore is in cyaniding form.

**Table 4. Preliminary results of microprobe analysis of gold and silver minerals from quartz-pyrite flotation concentrate of original ore**

No.	No. eds_sqt	Elements, weight ratio, %						Minerals
		Pb	Fe	S	Te	Au	Ag	
1	200					100.00		Pure gold
2	61					94.34	5.66	High-probe, almost pure Au
3	57				61.20		38.80	Hessite
4	98_10	35.92	12.30	13.00	30.70	8.00		Altaite and probably gold tellurides in galena
5	80_3		36.90	46.30	13.20	3.60		Gold tellurides in pyrite
6	99_11				71.00	29.00		Gold tellurides in pyrite
7	81_4				74.10	25.90		Gold tellurides in pyrite Excess of Te is found, Te is possible in native form
8	36				71.8	28.20		Gold telluride
9	39	Cu-2.30			71.5	25.40		Gold telluride and copper admixtures
10	199				88.84	11.16		Gold (or gold telluride) and sylvan in pyrite
11	202	22.04			48.83	Bi - 19.23	9.90	Mineral of radkligyte group PbBi <sub>2</sub> Te <sub>2</sub> – volynskite AgBiTe <sub>2</sub> ?

*Silver* accompanies gold; the average content of silver is 6.5 g/t. There were no silver minerals observed visually, though, silver fahlores, silver tellurides (telluric silver) and lead silver-bismuth telluride (radkligite group PbBi<sub>2</sub>Te<sub>2</sub> - volynskite AgBiTe<sub>2</sub>) were discovered during microprobe analysis. Silver associates with native gold and galena; it was observed in the form of admixtures in pyrite (two decimal places). It is supposed that the silver bulk is in the form of ultra-fine dispersed inclusions of native silver in sulfides and sulfosalts, which is indirectly confirmed by the results of scintillation and rational assaying. The silver is fine-grained and ultra-fine-grained according to the data of grain distribution analysis.

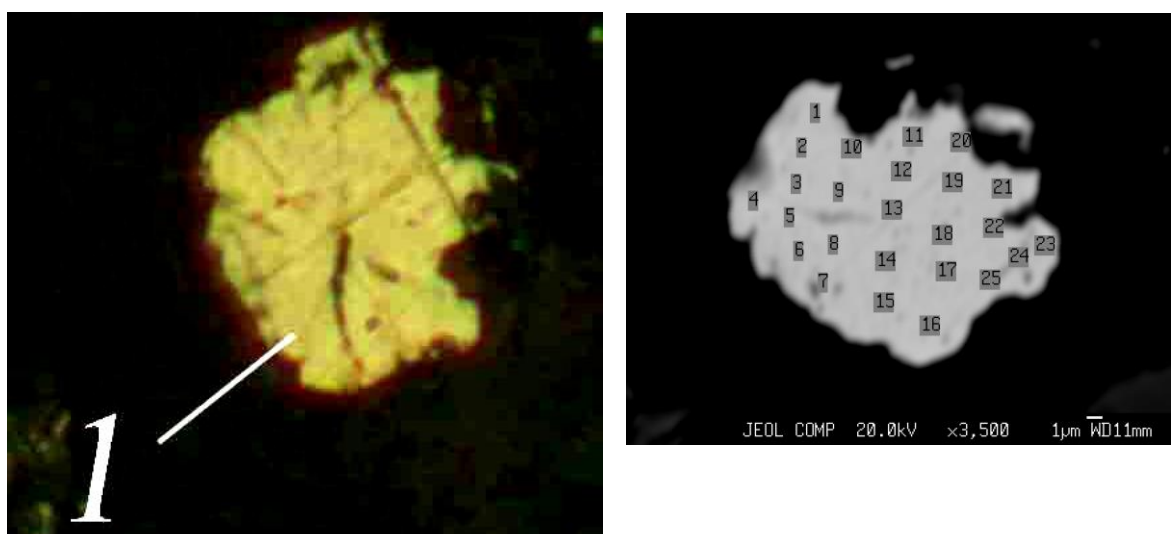


Fig. 12. Briquette polished section of quartz-sulfide flotation concentrate. A. Gold aggregate of 17 × 20 microns. Microscope. Nicholi II. Field of figure view is 40 microns. B. 1-25 - measuring points of composition. Backscattered electrons.

## Conclusion

In fact, argillized rocks of hydramicaceous facies with hydramicaceous illite prevailing in its composition are stated in the central part of the deposit that we have studied. Predominantly pyrophyllite-quartz metasomatic rocks develop above argillized rocks. It seems that pyrophyllite formed later than illite having replaced the latter; that means that argillization process typical for epithermal gold deposits was more previous and, obviously, pre-ore one. The synmineral stage of the studied site is characterized by pyrophyllite-quartz metasomatic rocks. Late hypogenous mica hydration process and further late carbonization processes seemingly occur at the post-ore stage.

Wall metasomatic rocks of Bereznyakovskoe deposit are typical for porphyry ore deposits. The same picture, for example, we may observe at Ikh Salaa gold molybdenum-copper-porphyry mineralization deposit (Central Mongolia); there we can observe propylitization with predominant albite-calcite-chlorite facies, argillization with predominant hydramica facies; ore mineralization areas are located in argillite development areas and are accompanied by quartz-sericite metasomatic rocks [Kulikova, Spiridonov, 2011].

Ore minerals of Bereznyakovskoe deposit are presented with gold, silver, pyrite, gray ores (tennantite, tetrahedrite, gray ore tellurides), sphalerite, galena, chalcopyrite, secondary copper sulfides, hydroxides of iron. The bulk of the ore minerals identified can be attributed to telluride-polymetallic stage (fahlore-telluride and gold-telluride substages). Some material of enargite and galena-sphalerite substages is present. The main part of the gold is found in native form, a minor part - in the form of gold tellurides. Often gold is in intergrowths with sulfides, sulfosalts, as well as with quartz, pyrophyllites, sericites, and illites.

*This work was financially supported by the project No. 02.G 25.31.0075 under the Decree of the Government of the Russian Federation No. 218 as of 09.04.2010.*

## List of references

1. Grabezhev A.I., Moloshag V.P. Mineralization of Tominsky copper-porphyry cluster // Report of the RAS, 1993, Vol.330, pp 349-351.
2. Grabezhev A.I., Sazonov V.N., Murzin V.V., Moloshag V.P., Sotnikov, V.I., Kuznetsov N.S., Puzhak B.A., Pokrosovsky B.G. Bereznyakovskoe gold deposit (Southern Urals, Russia) // Geology of ore deposits, 2000. No. 1, pp 38-52.
3. Korobeynikov A.F., Grabezhev A.I. Gold and platinum metals in copper-molybdenum-porphyry deposits // Bulletin of the Tomsk Polytechnic University, 2003. Vol.306, No. 5, pp 24-32.
4. Krivtsov A.I., Migachev I.F., Minina O.V. Mineralogical and geochemical types of porphyry copper ore deposits – gold bearing ability and zoning // Geochemistry, 1985. No. 10, pp 1417-1429.
5. Krivtsov A.I., Migachev I.F., Popov V.S. Porphyry-copper deposits of the world. Moscow, Science, 1986, pp 236.
6. Kulikova Z.I., Spiridonov A.M. Gold-containing molybdenum-copper-porphyry mineralization areas of Ikh Sala // Gold of North Pacific Rim, II International Mining and Geology Forum dedicated to the 110th anniversary of Yuri Bilibin. Abstracts of mining and geological conference. Magadan: NEISRI FEB RAS, 2011, pp 121-123.
7. Lodeyschikov V.V., Vasilyeva A.V. Methodical recommendations on classification of ores according to technological sampling and mapping of native gold deposits. Irkutsk: Irgiredmet JSC, 1997, pp 164.
8. Plotinskaya O.Y. Variations in composition fahlores of Bereznyakovskoe deposit (South Urals) // The role of mineralogy in the knowledge of the processes of mineralization. Proceedings of the annual session of the Mineralogical Society, dedicated to the 110th anniversary of the birth of Academician A.G. Betekhtin. Moscow: IGEM RAS, 2007, pp 257-260.

9. Plotinskaya O.Y., Novoselov K.A., Kovalenker V.A., Zeltman R. Variations of mineral forms of Au and Ag at Berezhnyakovskoe deposit (South Urals) // Modern methods of mineralogical and geochemical studies as a basis for identification of new types of ores and technologies of their integrated development. Materials of scientific conference "Annual Meeting of the Russian Mineralogical Society 2006". Edited by Marina Y.B. St.-Petersburg, 2007, pp 165-167.
10. Prokofyev V.Y., Bortnikov N.S., Zorina L.D. Gold porphyry deposits of the Mongolia-Okhotsk zone // New and innovative types of mineral deposits of Baikal and Transbaikal regions: Materials of All-Russian scientific-practical conference. Ulan-Ude: ECOS, 2010, pp 138-141.
11. Rusinov V.D., Kovalenker V.A., Matyusheva V.I., Naumov V.B. Zoning of ore deposition and metasomatism at Shtyavitsky ore field (Central Slovakia) // Geology of ore deposits, 1993, No. 3, pp 246-261.
12. Sazonov V.N., Murzin V.V., Grigoriev N.A. Berezhnyakovskoe gold porphyry deposit. Ekaterinburg: Ural Branch RAS, 1994, no pp.
13. Sazonov V.N., Murzin V.V., Grigoriev N.A. Vorontsovskoye gold ore deposit - an example of Carlin-type deposit in the Urals, Russia // Geology of ore deposits, 1998, No. 2, pp 157-170.
14. Taylor K.P. Oxygen and hydrogen isotopes in hydrothermal ore deposits // Geochemistry of hydrothermal ore deposits. Moscow: Mir, 1982, pp 200-232.
15. Bartos P.J. Prograde and retrograde base metal lode deposits and their relationships to underluingporphyry copper deposits // Econ. Geol., 1989. V. 84, № 6. P. 1671-1683.
16. Einaudi M.T. Environment of ore deposition at Cerro de Pasco, Peru // Econ. Geol., 1977. V. 77. P. 893-924.
17. Hedenquist J.W., Arribas A., Reynolds T.J. Evolution of an intrusion-centered hydrothermal system: Far Southiast-LepantoPorthyry and epithermal Cu-Au deposits, Philippins // Econ. Geol., 1998. V. 93. № 4. P. 373-404.
18. Hedenquist J.W., Izawa E., Arribas A., Whie N.C. Epithermal gold deposits: Styles, characteristics and exploration // Resource Geology special Publication. 1996. № 1.
19. Grabezhev A.I., Rusinova O.V., Zhukhlistov A.P., Murzin V.V. Vertikal ore-metasomatic of the Tominsk porphyry copper ore field (Southern Urals, Russia) // Geology of Ore Deposits. 1995. V. 37. № 6. P. 436-445.
20. Lehmann B, Heinhorst J, Hein U., Neumann M., Weisser J.D., Fedosejev V. The Berezhnyakovskoye gold trand southern Ural, Russia // Mineralium Deposita. 1999. V. 34. № 3. P. 241-249.
21. Lowell L.D., Guilbert J.M. Lateral and vertical alteration-mineralization zoning in porphyry ore deposits // Econ. Geol., 1970. V.65. № 3. P. 373-408.
22. Sillitoe R.N. The porphyry-epithermal transition // Report. Geol. Surv. Jap., 1992. V. 61. № 15. P. 3135-3144.